A machine learning approach for groundwater modeling

Mario G.C.A. Cimino
Dept. Information Engineering
University of Pisa
Pisa, Italy
mario.cimino@unipi.it

Manel Ennahedh
National Agronomic Institute of Tunisia
University of Carthage
Tunis, Tunisia
manel.nahedh@gmail.com

Federico A. Galatolo
Dept. Information Engineering
University of Pisa
Pisa, Italy
federico.galatolo@ing.unipi.it

Nejla Hariga-Tlatli
National Agronomic Institute of Tunisia
University of Carthage
Tunis, Tunisia
tlatli@topnet.tn

Issam Nouiri
National Agronomic Institute of Tunisia
University of Carthage
Tunis, Tunisia
issam.nouiri@inat.u-carthage.tn

Nicola Perilli
Dept. Civil and Industrial Engineering
University of Pisa
Pisa, Italy
nicola.perilli@unipi.it

Jamila Tarhouni
National Agronomic Institute of Tunisia
University of Carthage
Tunis, Tunisia
elmaainat@yahoo.fr

***Abstract*—This paper introduces a novel method and tools for groundwater modeling. The purpose is to perform numerical approximations of a groundwater system, for unlocking and paving water management problems and supporting decision-making processes. In the last decade, Data-driven Models (DdMs) have attracted increasing attention for their efficient development made possible by modern remote and ground sensing and learning technologies. With respect to conventional Process-driven Models (PdMs), based on mathematical modeling of core physical processes into a system of equations, a DdM requires less human effort and process-specific knowledge. The paper covers the design and simulation of a deep learning modeling tool based on Convolutional Neural Networks, integrated with the design and simulation of the workflow based on the Business Process Model and Notation (BPMN). Experimental results clearly show the potential of the novel approach for scientists and policy makers.**

Keywords—Groundwater flow, Numerical modeling, Workflow modeling, Deep Learning

I. Introduction and Background

Groundwater modeling is a computational method to perform numerical approximations of a groundwater system, for addressing water management problems and supporting decision-making processes. Typical uses of groundwater models are what-if analysis and forecasting [1]. Groundwater systems are affected by past, current, local, global, natural and anthropogenic impacts. Their modeling is based on knowledge, information and data related to a range of factors. The observation of characteristics, the conceptual understanding of relevant phenomena, the gathering and monitoring of spatio-temporal data are fundamental for a deep understanding of the system and the proxy parameters for limiting the model uncertainty [2]. The workflow of conventional groundwater modeling takes a long time and a huge human time-consuming effort. In particular, a *Process-driven Model* (PdM) is the formal description of the core physical processes into a system of governing equations. The governing equations are usually solved numerically, deriving a discrete solution in the space and time. A PdM is based on deep knowledge of the observed system dynamics. It requires many additional spatial data on geological features and hydrogeological properties of the aquifer. Large computational resources and long calibration activities are due for the increasing refinement and complexity of a PdM [3].

In the last decade, *Data-driven Models* (DdM) have attracted increasing attention for their optimized development made possible by modern sensing and deep-learning technologies. A DdM requires a different approach, based on systematic data acquisition and low process-specific knowledge, which is incorporated as data transformation into features. For example, to predict groundwater levels, the input data could be: historical piezometric data and surface water levels, climatic data, land-use/land cover, groundwater withdrawal and socio-economic data [4]. The generated model captures the underlying input-output mapping without additional expert user input. In particular, Deep Learning (DL) an engineered machine learning, made possible by Graphical Processing Units (GPUs), can model large data sets with a sensibly reduced human effort with respect to conventional machine learning. PdM and DdM can actually be combined for achieving a better potential. For example, an input-output mapping can support process-oriented modeling and understanding, as well as process-oriented modeling can determine the best feature engineering for input-output mapping [5]. According to this perspective, the objective of this work is to explore and measure the effectiveness of DdM versus PdM, developing a particular DL architecture for a case study, as well as an operational workflow to measure the productivity of both approaches. The selected case study is the strategic aquifer of the Mornag Plain (Tunisia), affected by a massive withdrawal of groundwater mainly for irrigation purposes.

As a DL architecture, a *Convolutional Neural Network* (CNN) will be developed. In a CNN, objects are recognized via local and global features, i.e., based on simple patterns and on more structured patterns, respectively. In particular, a CNN is the state-of-the art DL solution to exploit the local topological nature of features in the groundwater maps. A CNN has the advantage that it does not need hand-engineered filters based on prior knowledge and human effort, with respect to traditional data processing algorithms. This means that by providing the set of input-output data, an optimization (training) algorithm is able to iteratively modify the network parameters in order to reduce the output error, i.e., to provide

XXX-X-XXXX-XXXX-X/XX/$XX.00 ©20XX IEEE

a numerical value very close to the target. Moreover, the model can be general, i.e., the network is able to effectively provide the output for new data. A very important aspect of DL modeling is to select the best hyperparameters of the architecture. An example of hyperparameter is the learning rate, i.e., the speed at which the network learns. A too small value can produce a very long training process that could get stuck, whereas a too large value can produce an unstable training process. In order to guarantee the reproducibility of the training, the most sensitive hyperparameters are not set by hand, but using an automatic optimization algorithm.

The remainder of this paper is organized as follows: Section II defines the workflow of ground water modeling via PdM and DdM. Section III covers the case study. Section IV summarizes the development of the DL architecture. Finally, Section V draws conclusions, future challenges and works.

II. The workflow of groundwater modeling

Fig. 1 shows the workflow of the groundwater PdM, in a standard graphical representation called Business Process Model and Notation (BPMN). The BPMN has been developed with a solid mathematical foundation, to allow execution, simulation, and automation of consistency checking [6]. It is also suitable to standardize and facilitate the communication between all stakeholders. In BPMN, an event, an activity, a decision/merge node are represented by a circle, a rounded box, a diamond, respectively. Sequence flow and data flow are represented by solid and dotted arrows, respectively. Finally, data storage is represented by a cylinder.

In particular, the workflow starts when there is a new model to generate (event on top-left). When new data are available, the first activity is the ingestion of hydrogeological and geological data, made by: (i) discharge/recharge sources, (ii) piezometric data, (iii) hydrodynamic parameters, and (iv) acquifer geometry & boundary conditions. If the ingested data are sufficient, two parallel tasks are carried out: on one side, the generation of sensor data from discharge/recharge sources and piezometric data; on the other side, the generation of geographic map. The human icon on the task means that the activity is managed by a human and not fully automated. Subsequently, the generation of thematic maps via GIS (Geographic Information System) is performed, followed by the generation of a conceptual model via the Groundwater Modeling System (GMS) software. If the model is completely new, a grid is set, and then computed. Then the hydrogeologic model can be simulated using hydrodynamic parameters. Finally, the model is calibrated, using observed piezometric data and providing discharge/recharge sources. If the model is not sufficiently accurate, then the workflow restarts from the generation of the thematic maps (hydrodynamic parameters and discharge/recharge sources).

Fig. 2 shows the workflow of the groundwater DdM. What is different is the sequence of the last three tasks: optimize hyperparameters, train the model, and assess model accuracy. In case of inaccurate model, only the last three tasks are repeated. Table I shows the simulation parameters for the workflow of both PdM and DdM. The simulation has been carried out via the BIMP simulator [7]. Fig. 3 and Fig. 4 show the average number of executions over 10 runs, for both PdM and DdM, represented in a color scale. Specifically, it is apparent that the major costs associated to the PdM are related to the calibration loop, which is colored in red because it is executed on average 17.2 times. In contrast, the hyperparameters optimization loop of the DdM is carried out on average 1.1 times. Not surprisingly, Fig. 5 and Fig. 6 show the average duration of each task: here the calibration task takes the highest time in PdM, and the ingestion task in DdM. Overall, the average time for each instance of process, in the PdM and DdM, is 13.2 months and 52.5 days, respectively. This result clearly shows the advantages of DL in the chain.

III. The case study of the Mornag Plain aquifer

The selected study case is the well-know Mornag Aquifer, located in the north east of Tunisia characterized by a semi-arid climate. The rich agricultural Mornag coastal plain, lies 20 Km SE of Tunis (Fig. 7). Vineyard and olive tree are the main crops, and irrigation is secured by groundwater hosted within the clastic aquifer and surface sources. Treated wastewater for multi-reuse including irrigation are also provided by local wastewater treatment plants [8]. Groundwater is the most important water source in Mornag for agriculture, domestic, and industry uses. To manage the negative effects of groundwater level decline and help decision-making in water management, a numerical simulation based on an integrated GIS-GMS has been adopted. Simulation allows to understand the groundwater flow dynamic and to assess the functioning of the aquifer system in the Mornag Plain [9][10].

TABLE I. Groundwater model simulation parameters

Simulation model parameter	Value
Duration of *ingest hydrogeologic data*	83.3 – 96.7 days
Duration of *generate sensor data*	1.0 – 2.0 hours
Duration of *generate geographic map*	30.0 – 60.0 days
Duration of *generate thematic map via GIS*	27.9 – 37.3 days
Duration of *generate conceptual model via GMS*	27.1 – 35.4 days
Duration of *set grid*	1.0 – 2.0 hours
Duration of *(re-)compute grid*	24 – 48 hours
Duration of *simulate hydrogeologic model*	26.3 – 34.6 days
Duration of *calibrate hydrogeologic model*	90 – 150 days
Duration of *optimize hyperparameters*	2.0 – 4-0 hours
Duration of *train the model*	0.3 – 0.6 hours
Duration of *assess model accuracy*	0.3 – 0.6 hours
Percentage of *sufficient data*	95%
Percentage of *existing grid*	95%
Percentage of *model accurate* (PdM)	5%
Percentage of *model accurate* (DdM)	95%

The main step of the groundwater modeling process is to develop the conceptual model, by combining all thematic maps (aquifer geometry, boundary conditions, hydrodynamic parameters, discharge/recharge sources, and piezometric data). All thematic maps were integrated into the GMS using the GIS environment. The conceptual model helps for a better understanding of the aquifer system behaviors and tunes the groundwater modeling [9]. After spatio-temporal discretization, setting of the initial values, partition of the hydrodynamic parameters, disposal of the sources and sinks, the 3D model was simulated using the finite-difference code, MODFLOW (Fig. 8).

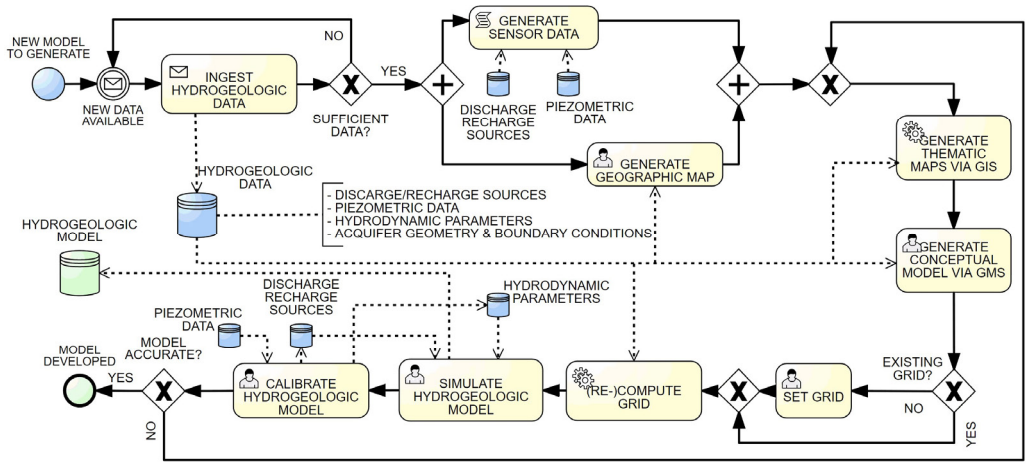

Fig. 1. BPMN workflow of groundwater Process-driven Modeling.

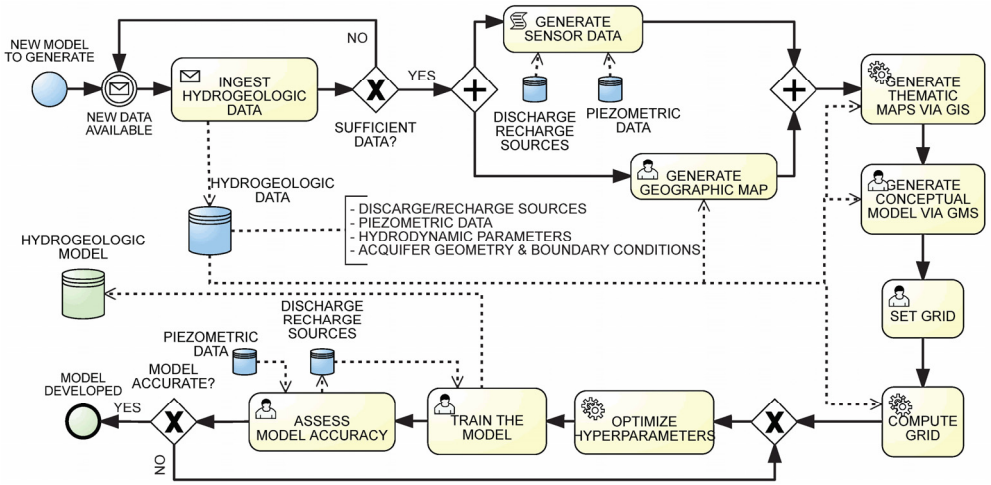

Fig. 2. BPMN workflow of groundwater Data-driven Modeling.

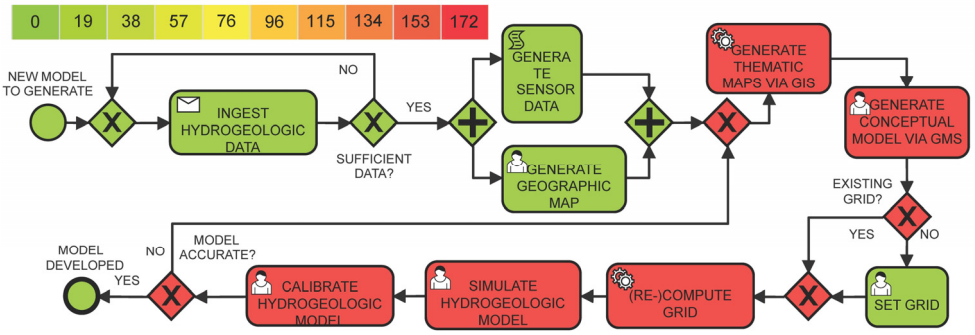

Fig. 3. Heatmap based on counts for Process-driven Modeling

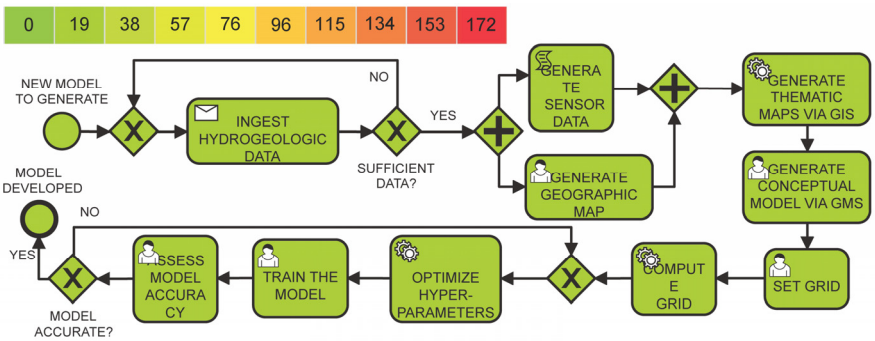

Fig. 4. Heatmap based on counts for Data-driven Modeling

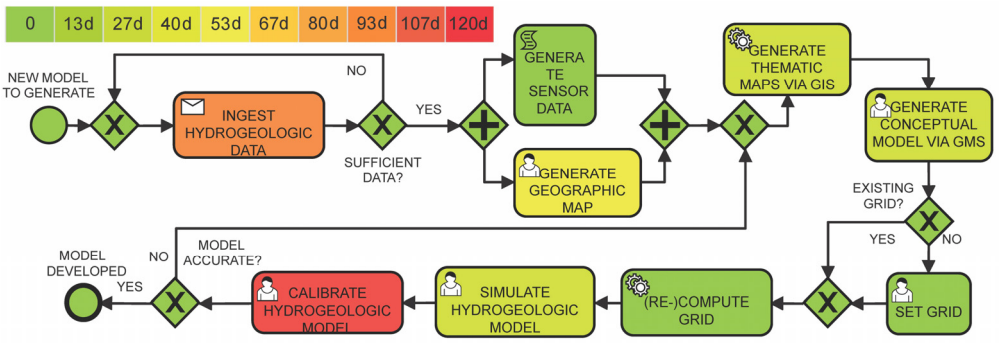

Fig. 5. Heatmap based on durations for Process-driven Modeling

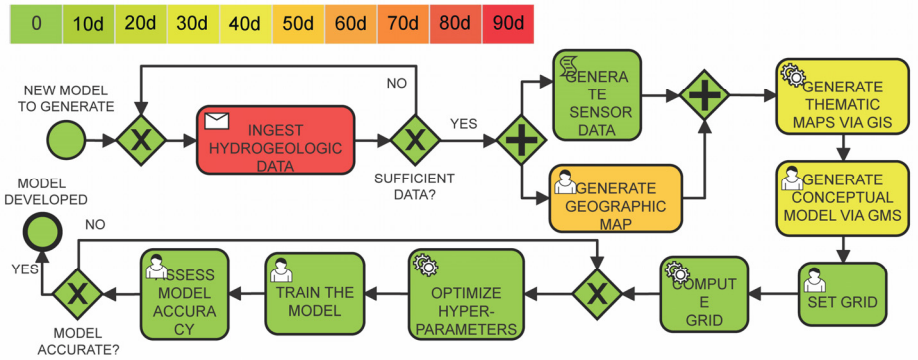

Fig. 6. Heatmap based on durations for Data-driven Modeling

Fig. 7. The general location map of the study area (via GIS)

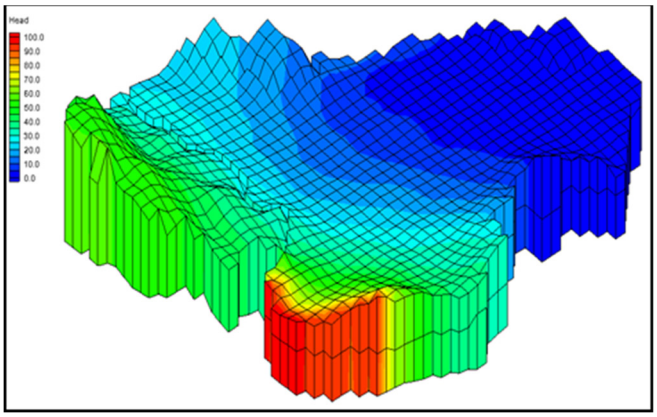

Fig. 8. 3D shape of the Mornag aquifer model calibrated (via GMS).

An important step is calibration. During iterative process, the input parameters to a groundwater model are modified to ensure that the conceptual model matches the real hydrogeological situation. It is mainly reflected in the fact that the simulated piezometric level is consistent with the observed piezometric level (fitting error of the long-time observation well was within the confidence interval) [9]. The steady-state model was calibrated with the hydrological conditions of the year 1971 when the hydraulic heads were appeared to be in equilibrium condition [11]. Transient simulations were calibrated for two stress periods, namely the winter and summer stress periods, for each year between 1971 and 2015. As a result, from the numerical simulation of the Mornag aquifer system, we note that the applied method (MODFLOW simulation) can reflect the changes within the input and output of the groundwater system (simulated piezometric level), with the flexibility to acknowledge physical significance (parameter estimation) and predict the output changes under different hydrological dynamic conditions. Nevertheless, the spatially and temporally variable parameters and inputs to complex groundwater models typically end in long runtimes which hinder comprehensive calibration, sensitivity, and uncertainty analysis. There are thus deficiencies in satisfying the necessities of high precision and dynamic management [12]. The PdM is calibrated using 80% of the data, and validated with the remaining 20%. Overall, the Mean Absolute Residual (MAR) of the hydraulic head level error achieved is 4.84 meters [13].

IV. Development of the Data-driven Model

The proposed architectural model has been implemented, tested, and publicly released with the dataset on the Github platform [14], to foster its application on various research environments. In particular, the DL architecture takes as inputs the *recharge rate* (Fig. 9), *river level*, and *pumping wells* (Fig. 10), and provides as outputs the *flow front face*, *flow lower face*, *flow right face*, *hydraulic head level*, and *storage*. The dataset is made by 88 samples. Each sample

represents a period of 6 months, from 1971 to 2015, and is made by a grid of 725 cells (41×50), corresponding to an area of 182 Km^2.

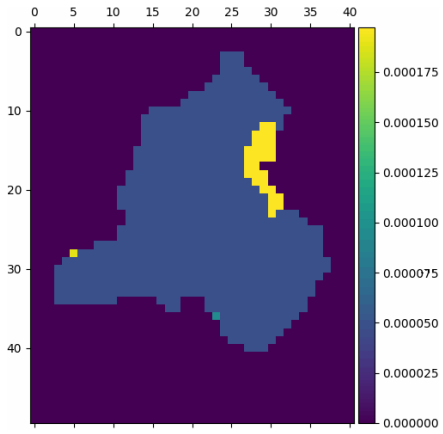

Fig. 9. Sample input (recharge rate).

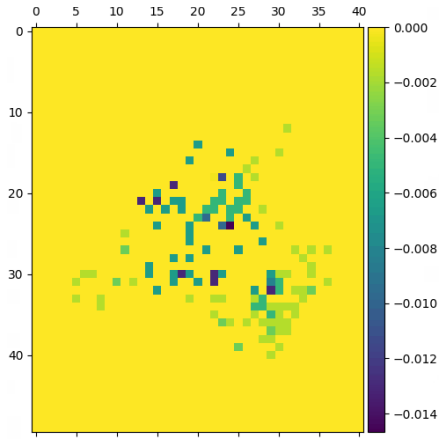

Fig. 10. Sample input (pumping wells).

The overall architecture is structured as follows. For each of the three inputs, an independent CNN is used for feature extraction [15]. Then, an encoding Feed Forward Neural Network (FFNN) takes the three features provided by each CNN, and provides an encoded output. Such output feeds five Transpose CNN (TCNN), for corresponding five outputs. The CNN is structured as follows: batch normalization and two subsequent layers, each made by convolutional layer with kernel size 5×5, a max pool layer with size 3×3, and a leaky ReLU activation function. The structure of the encoding FFNN is made of two layers of neurons, each layer size is established by the hyperparameter optimization process (a typical value is about 180 neurons). The TCNN is structured as follows: two subsequent layers, each made by convolutional transpose layer followed by a ReLU activation function. The first layer with kernel size 5×5 and dilation 2, and the second layer with kernel size 7×7 and dilation 2. Finally, a convolutional transpose layer with kernel size 10×10 and dilation 3. The dataset is partitioned with the holdout method in training (60%), validation (20%) and testing (20%).

To guarantee the reproducibility of the training, the most sensitive hyperparameters have been set using an optimization algorithm based on a Tree Parzen Estimator (TPE) for determining the best choice [16]. On average, the hyperparameter optimization has been carried out in 3.52 hours, using the following hardware resources: GPU *NVIDIA™ GeForce RTX 2080*; CPU *Intel® Core™ i9-9900K @ 3.60GHz*; CACHE L1 *512 KB*, L2 *2 MB*, L3 *16 MB*. On average, a training is carried out in 9.67 mins. Fig. 11 shows the average Mean Squared Error (MSE), i.e., computed over the five outputs, against the number of iterations, in the hyperparameters optimization process. As a result, the following best hyperparameters values have been found: learning rate: 0.00159, batch size: 32, patience: 50, loss: L1, features size: 49, CNN channels: 5 (1st level), 10 (2nd level), TCNN channels: 20 (1st level), 20 (2nd level). Fig. 12 shows the average MSE, i.e., computed over the five outputs, against the number of iterations, for the training and validation errors made with the best hyperparameters. The learning curve is characterized by a good fit model, because it starts with moderately high training and validation errors, then gradually decreases and flattens. Moreover, both the training and validation errors move close to each other, with validation being slightly greater than the training error.

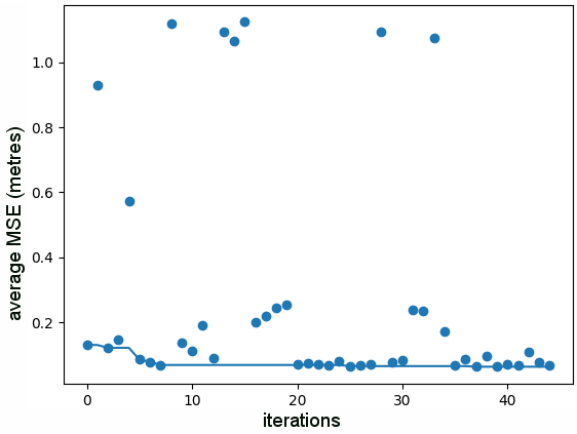

Fig. 11. Average MSE (meters) against number of iterations in the hyperparameters optimization process.

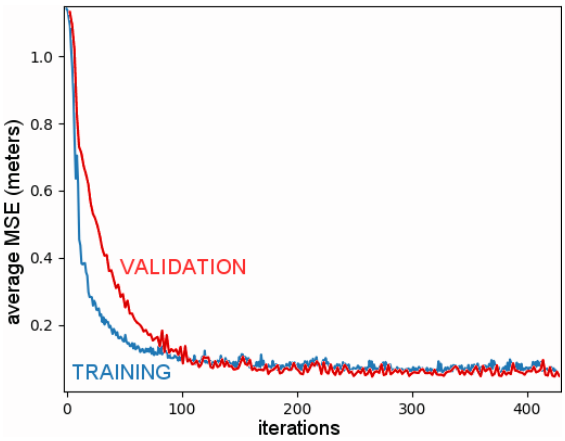

Fig. 12. Average MSE (meters) of training and validation errors against number of iterations.

Table II shows the Mean Absolute Error of the output provided by the Data-driven Model, for the training, validation and testing processes. Here, the different sizes are due to the different scales of each output. In particular, it is worth to note that the error on hydraulic head level is about 0.32 meters, which is very promising considering the hydraulic head level error achieved by the Process-driven Model, i.e., 4.84 meters. For a better insight, Fig. 9, Fig. 10, and Fig. 13 show a sample input of recharge and wells provided to the model, with the related head output (a), target (b) and absolute error (c).

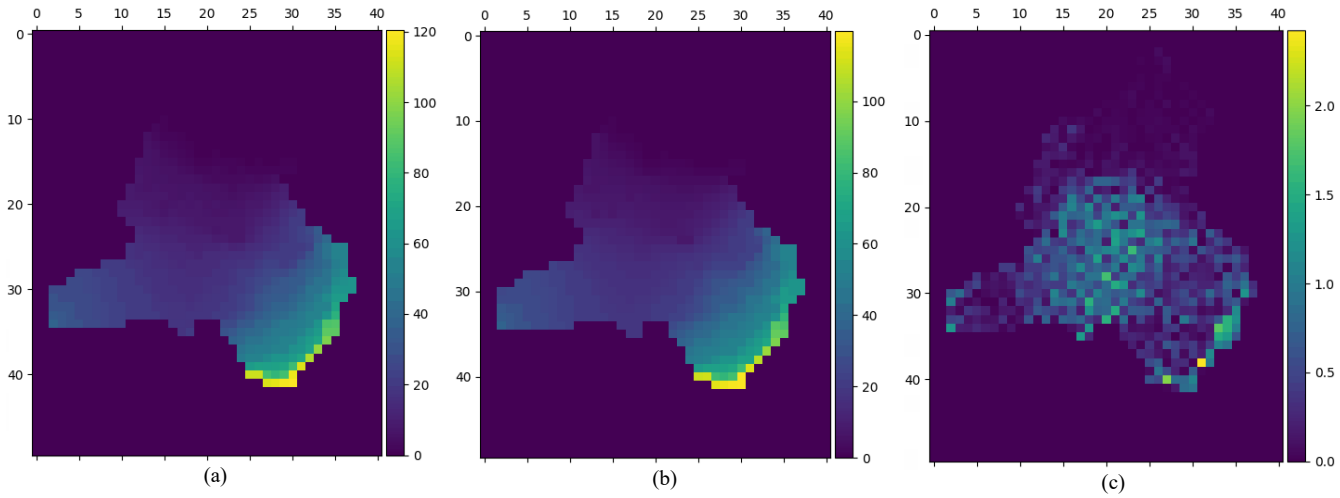

Fig. 13. Sample hydraulic head level: output (a), target (b), absolute error (c).

TABLE II. PERFORMANCE OF THE DATA-DRIVEN MODEL

Output	Training MAE (mt.)	Validation MAE (mt.)	Testing MAE (mt.)
Flow front face	0.000287	0.000320	0.000305
Flow lower face	1.626	2.365	1.794
Flow right face	0.000242	0.000255	0.000248
Hydraulic head level	0.319	0.320	0.329
Storage	0.000160	0.000185	0.000163
Average	**0.0639**	**0.0641**	**0.0659**

V. CONCLUSIONS AND FUTURE WORK

Data-driven models and the related workflow models offer a new perspective to groundwater modeling useful for scientists, policy makers and water users. According to this perspective, this work explores and measures the effectiveness of a data-driven modeling method, developed with a Deep-Learning architecture on a real-world case study, as well as an operational workflow to measure its productivity compared with a conventional process-driven approach. As a case study, the Mornag Plain aquifer is considered. Overall, the proposed method is able to achieve an absolute error on hydraulic head level of 0.32 meters, which is very accurate with respect to the error of 4.84 meters provided by a traditional approach. In terms of workflow efficiency, the average duration of the data-driven modeling is 52.5 days, which is very fast with respect to the average duration of 13.2 months for the traditional workflow. Given such promising results, the future works will focus on more experimentation of the proposed method for a new stream of data, to understand the variations in hydraulic head level and how it is affected by the changes in hydrological conditions under the context of the climate change (recharge rate and pumping wells).

ACKNOWLEDGMENTS

Work supported by: (i) the Italian Ministry of Education and Research (MIUR) in the framework of the CrossLab project (Departments of Excellence); (ii) the Tunisian Ministry of Higher Education and Scientific Research.

REFERENCES

[1] Mary P. Anderson, William W. Woessner, Randall J. Hunt, Applied Groundwater Modeling (Second Edition), Academic Press, (2015).

[2] Mathias, S., & Wheater, H. Groundwater modelling in arid and semi-arid areas: An introduction. In H. Wheater, S. Mathias, & X. Li (Eds.), Groundwater Modelling in Arid and Semi-Arid Areas (International Hydrology Series, pp. 1-4). Cambridge University Press. (2010).

[3] Chen, C., He, W., Zhou, H. et al. A comparative study among machine learning and numerical models for simulating groundwater dynamics in the Heihe River Basin, northwestern China. Sci Rep 10, 3904 (2020).

[4] Kenda K, Čerin M, Bogataj M, Senožetnik M, Klemen K, Pergar P, Laspidou C, Mladenić D. Groundwater Modeling with Machine Learning Techniques: Ljubljana polje Aquifer. Proceedings. 2018; 2(11):697.

[5] Asher, M. J., Croke, B. F. W., Jakeman, A. J., & Peeters, L. J. M. (2015). A review of surrogate models and their application to groundwater modeling. *Water Resources Research, 51*(8), 5957-5973.

[6] Cimino, M.G.C.A., Palumbo, F., Vaglini, G. *et al*. Evaluating the impact of smart technologies on harbor's logistics via BPMN modeling and simulation. Inf Technol Manag 18, 223–239 (2017).

[7] BIMP Simulator, QBP, https://bimp.cs.ut.ee/simulator, 2021.

[8] Brahim-Neji, H., F. Jarraya-Horriche, and F. Slama, Multicriteria decision aid for choosing groundwater artificial recharge sites with treated wastewater: Case study of Mornag aquifer. 2017.

[9] Karimi, L., Motagh, M., and Entezam, I. (2019), 'Modeling groundwater level fluctuations in Tehran aquifer: Results from a 3D unconfined aquifer model', Groundwater for Sustainable Development, 8, 439-49.

[10] Sudhakar, S, et al. (2016), 'Application of GIS and MODFLOW to ground water hydrology–a review', 6 (1), 36-42.

[11] Ennabli, M., Etude hydrogéologique des aquifères du Nord-Est de la Tunisie pour une gestion intégrée des ressources en eau. 1980, Nice university: Paris. p. 171.

[12] Asher, M. J., Croke, B. F. W., Jakeman, A. J., & Peeters, L. J. M. (2015). A review of surrogate models and their application to groundwater modeling. Water Resources Research, 51(8), 5957-5973.

[13] Ennahedh, M., Hariga-Tlatli, N., & Tarhouni, J. (2020). Hydrogeological modeling for the aquifer system of the Mornag Plain for future real-time management. Paper presented at the t3rd Conference of the Arabian Journal of Geosciences (CAJG 2020), Sousse, Tunisia.

[14] Galatolo, F.A., Setit2022 Github repository, (2021). URL: https://github.com/galatolofederico/setit2022.

[15] Federico A Galatolo, Mario G C A Cimino, Gigliola Vaglini, "Generating Images from Caption and Vice Versa via CLIP-Guided Generative Latent Space Search", Proceedings of the Int. Conf. on Image Processing and Vision Engineering, 1:166-174 (2021).

[16] Bergstra, J., Bardenet, R., Bengio, Y., Kégl, B.: Algorithms for hyperparameter optimization. Advances in neural information processing systems 24 (2011).